

# Materials Research Express



## PAPER




# Biosynthesis of gold and silver nanoparticles using *Parkinsonia florida* leaf extract and antimicrobial activity of silver nanoparticles

RECEIVED  
12 February 2019

REVISED  
31 May 2019

ACCEPTED FOR PUBLICATION  
27 June 2019

PUBLISHED  
5 July 2019

Alejandra López-Millán<sup>1</sup>, Carmen Lizette Del Toro-Sánchez<sup>2</sup>, José Rogelio Ramos-Enríquez<sup>3</sup>, Roberto Carlos Carrillo-Torres<sup>1</sup> , Paul Zavala-Rivera<sup>1,4</sup>, Reynaldo Esquivel<sup>1</sup> , Enrique Álvarez-Ramos<sup>1</sup>, Ramón Moreno-Corral<sup>5</sup>, Roberto Guzmán-Zamudio<sup>1,6</sup> and Armando Lucero-Acuña<sup>1,4,6,7</sup> 

<sup>1</sup> Nanotechnology Graduate Program, Department of Physics, University of Sonora, Hermosillo 83000, Sonora, Mexico

<sup>2</sup> Research and Graduate in Food Department, University of Sonora, Hermosillo 83000, Sonora, México

<sup>3</sup> Department of Chemistry-Biology, University of Sonora, Hermosillo 83000, Sonora, México

<sup>4</sup> Department of Chemical and Metallurgical Engineering, University of Sonora, Hermosillo 83000, Sonora, Mexico

<sup>5</sup> Department of Polymers and Materials, University of Sonora, Hermosillo 83000, Sonora, Mexico

<sup>6</sup> Department of Chemical and Environmental Engineering, University of Arizona, Tucson 85721, Arizona, United States of America

<sup>7</sup> Author to whom any correspondence should be addressed

E-mail: [armando.lucero@unison.mx](mailto:armando.lucero@unison.mx)

**Keywords:** green chemistry, silver nanoparticles, gold nanoparticles, antibacterial activity, parkinsonia florida

Supplementary material for this article is available [online](#)

## Abstract

In this work, the biosynthesis of gold and silver nanoparticles from a leaf extract of *Parkinsonia florida* (*P. florida*) is reported. The *P. florida* leaf extract was analyzed by a phytochemical screening, by measuring the DPPH radical scavenging activity, and by Fourier-transform infrared spectroscopy (FT-IR). The phytochemical screening results indicated that biomolecules like carbohydrates, phenols, proteins, aminoacids, saponins, and flavonoids present in *P. florida* leaf extract might have participated in the chemical reduction of the metallic salts and further colloidal stabilization. The FT-IR results from leaf extract functional groups support the role of surface modification with the presence of residues of phenols, proteins, aminoacids, saponins, and flavonoids. The formation of metallic nanoparticles was confirmed by optical absorption spectroscopy with characteristic absorption bands at 550 nm and 430 nm, for gold and silver nanoparticles, respectively. Zeta potential for gold nanoparticles presents negative values in the range of  $-10 \pm 1$  to  $-16 \pm 1$  mV, depending on the amount of leaf extract used during the synthesis reaction. Similarly, zeta potential values for silver nanoparticles were in the range of  $-5 \pm 1$  to  $-16 \pm 1$  mV. STEM images revealed the average particles sizes in the range from 10 to 15 nm, and 10 to 57 nm, for gold and silver nanoparticles respectively. The silver nanoparticles presented good antibacterial activity, inhibiting the growth of *Staphylococcus aureus* and *Escherichia coli*.

## 1. Introduction

The methods for metallic nanoparticle synthesis are widely investigated due to their potential applications in diverse areas. The main methods to synthesize nanoparticles include chemical and physical pathways [1–4], but sometimes these routes are expensive and environmentally harmful. Green synthesis methods avoid these complications by achieving the synthesis of nanoparticles with plants extracts or microorganisms [4–8]. The formation of metallic nanoparticles by natural sources, like plant extracts, is supported by the presence of molecules such as carbohydrates, proteins, aminoacids, phenols, flavonoids, terpenoids, alkaloids, and many others that can be capable of carrying out the reduction of metal ions [9, 10]. The extraction of the active molecules of interest of a plant involves the separation of active portions that are present in leaves, flower, root, among others, using specially selected solvents and standardized methods. Usually, the final product obtained from the extraction is a relatively complex mixture of active molecules. Naturally, the presence of these

molecules, responsible for the reduction of the metal ions, can be very different from sample to sample [8]. The synthesis of metallic nanoparticles using plant extracts (leaf, bark, stem, root, etc), could be obtained by mixing the extract with a metallic salt solution, where the chemical reduction of the salts into nanoparticles can be made without external stabilizing/capping agents and at room temperature [10–12].

Green synthesis of gold nanoparticles has been reported using aqueous seed extract of *Abelmoschus esculentus* [13], Neem leaves extract [14], *Salvia officinalis*, *Lippia citriodora*, *Pelargonium graveolens* and *Punica granatum* [15], *Hibiscus Tiliaceus* plant [16], *Indigofera tinctoria* leaf extract [17], among others. Gold nanoparticles applications include targeted drug delivery [18], gene delivery [19], antitumor and cancer therapy [17, 20–22], bio-imaging [23, 24] and other potential applications [25]. On the other hand, the green synthesis of silver nanoparticles (AgNPs) has been reported using an aqueous extract of Neem [26], banana peel extract [28], *Trianthema decandra* extract [29], *Abutilon indicum* leaf extract [30], *Psidium guajava* L. leaf extract [31], among others. Additionally, silver nanoparticles present antibacterial activity against both, Gram-negative and Gram-positive bacteria, being the first more sensitive [8, 32] due to the difference in structural characteristics of the bacterial species.

*Parkinsonia florida* (*P. florida*), usually called *Cercidium floridum* or blue paloverde, is a tree of the *Caesalpinioideae* sub-family [33, 34], also known as peacock family (*Leguminosae*), which comprises approximately 180 genres and approximately 3000 species. It includes many economically important legumes like *Bauhinia forficata*, *Caesalpinia gilliesii*, *Caesalpinia spinosa*, *Ceratonia siliqua*, *Cercis siliquastrum*, *Gleditsia triacanthos*, *Gymnocladus dioica*, *Parkinsonia aculeata*, and *Senna multiglandulosa* [35]. *P. florida* is found mainly in the Colorado desert, the southeast of California, the Sonora desert, southern Arizona, and in the northwest of the state of Sonora (Mexico). *Parkinsonia* spp. contains potent antioxidants and phytochemicals in flowers, leaves, and stems like glycosides, flavonoids, sterols, and minerals. The leaves also contain C-glycosyl flavones like orientin, vitexin, and iso-vitexin, Parkinsonin A, Parkinsonin B, and Parkintin [33, 37].

In this work, *P. florida* leaf extract is used as a reducing and capping agent in the synthesis of gold and silver nanoparticles, while tetrachloroauric acid and silver nitrate are used as precursors. Phytochemical screening of *P. florida* leaf extract is presented, and the obtained metallic nanoparticles are characterized by Fourier-transform infrared spectroscopy (FT-IR), optical absorption spectroscopy, scanning transmission electron microscopy (STEM), and zeta potential. The antimicrobial activity of silver nanoparticles is evaluated against Gram-positive and Gram-negative bacteria.

## 2. Materials and methods

### 2.1. Materials

Tetrachloroauric (III) acid ( $\text{HAuCl}_4$ ), silver nitrate 99% ( $\text{AgNO}_3$ ), ferric chloride ( $\text{FeCl}_3$ ), 2,2-diphenyl-1-picrylhydrazyl (DPPH), 6-hydroxy-2,5,7,8-tetramethylchroman-2-carboxylic acid (Trolox) and sulfuric acid ( $\text{H}_2\text{SO}_4$ ) were purchased from Sigma-Aldrich (St. Louis, MO, USA). Nitric acid ( $\text{HNO}_3$ ), hydrochloric acid (HCl) and glacial acetic acid ( $\text{CH}_3\text{COOH}$ ) were purchased from Fermont (Monterrey, N L México). Antibiotic Disks of tetracycline and vancomycin were purchased from Becton Dickinson (Sparks, MD, USA), Mueller-Hinton Agar (MHA), mannitol salt and eosin methylene blue (EMB) agar were purchased from MCD LAB (Tlalnepantla, Edo de México). Culture cells of *Escherichia coli* ATCC 25922 and *Staphylococcus aureus* ATCC 25923 were proportioned by the microbiology laboratory of the University of Sonora.

### 2.2. Leaf extract preparation

*P. florida* leaf extract was used to prepare metallic nanoparticles adapting well-known literature methods of extraction [38]. Briefly, fresh leaves were collected from the University of Sonora campus (Hermosillo, Sonora, Mexico) (Latitude 29.081890, Longitude  $-110.959947$ ) in April, November, and January. They were surface-cleaned with running tap water and distilled water to remove debris and other contaminated organic contents. Then, the clean leaves were air-dried at room temperature for 2 h. Next, 3 g of finely cut dry leaves were kept in a flask glass containing 100 ml deionized water and boiled during 30 min. The extract was cooled down and filtered with Whatman filter paper no.1, and the extract was stored at 4 °C for further use. A small volume of extract was freeze-dried for further analysis.

### 2.3. Phytochemical screening of leaf extract

The phytochemical characteristics of *P. florida* extract were investigated for the presence of carbohydrates, alkaloids, saponins, proteins, phenol, flavonoids and cardiac glycosides following standard biochemical methods [38]. Additionally, FT-IR measurements were carried out by attenuated total reflectance (ATR) using a Spectrum Two FT-IR spectrometer (Perkin-Elmer), placing the lyophilized samples directly onto the ATR crystal, and the spectrum was collected in the 4000–500  $\text{cm}^{-1}$  interval with a resolution of 4  $\text{cm}^{-1}$ .

#### 2.4. DPPH free radical scavenging assay

The antioxidant activity of *P. florida* extracts was evaluated by the DPPH free radical method previously reported by Cheel *et al*, with some modifications [39]. The assay is based on the differences of absorbance produced by the reaction of DPPH free radical with H-donors of the extract. Briefly, 200  $\mu\text{l}$  of a 6.34  $\mu\text{M}$  DPPH methanolic solution were added to 20  $\mu\text{l}$  of *P. florida* extract at various concentrations (125, 250, 500, 1000, 2000  $\mu\text{g ml}^{-1}$ ) in a 96-well plate (Costar Corning NY the USA). The plates were incubated with agitation for 30 min in the dark at room temperature. Then, the absorbance was measured at 515 nm in a microplate reader. Trolox was used as a control, and a mixture of methanol and DPPH was used as a blank. The degree of discoloration is proportional to the efficiency of the extract. The percentage of discoloration (inhibitory effect, IE%) is calculated from the percentage of the difference between the absorbance of the control and the sample over the absorbance of the control, and results are reported as Trolox equivalents. Tests were performed in triplicate.

#### 2.5. Synthesis of silver nanoparticles

Silver nanoparticles (AgNPs) were synthesized by adapting literature methods of green synthesis [8, 40]. Briefly, 10 ml of 0.1 M  $\text{AgNO}_3$  stock solution was prepared. Then, silver nitrate was mixed with different concentrations of *P. florida* leaf extract (4.35, 8.70, 13.05, 17.4 and 21.5  $\mu\text{g ml}^{-1}$  of equivalent Trolox), keeping constant the final concentration of silver nitrate at 0.2 mM. The mixture was left to react at room temperature for 24 h. Finally, AgNPs were washed by centrifugation at 5000 rpm ( $2598 \times g$ ) for 20 min and resuspended in deionized (DI) water. An aliquot of the purified suspension was lyophilized and analyzed by FT-IR. The remaining purified suspension was maintained at room temperature and analyzed during several weeks.

#### 2.6. Synthesis of gold nanoparticles

Gold nanoparticles (AuNPs) were synthesized in a similar way than silver nanoparticles. Different amounts of a stock solution of  $\text{HAuCl}_4$  0.01 wt% were mixed with *P. florida* extract with 4.35, 8.70, 13.05, 17.4 and 21.5  $\mu\text{g ml}^{-1}$  of equivalent Trolox and left to react during 24 h, keeping constant the final concentration of gold (2 mM). Finally, AuNPs were washed by centrifugation at 5000 rpm ( $2598 \times g$ ) for 20 min and resuspended in DI water. An aliquot of the purified suspension was lyophilized and analyzed by FT-IR. The remaining purified suspension was maintained at room temperature and analyzed during several weeks.

#### 2.7. Nanoparticle characterization

The obtained nanoparticles were characterized by scanning transmission electron microscopy (STEM) using a JEOL JSM-7800F field-emission scanning electron microscope equipped with a STEM detector (Deben UK Ltd, London). Samples were immobilized on carbon-coated copper grids. Colloidal stability was evaluated by measuring zeta potential of the nanoparticles, using a Malvern ZetaSizer Nano ZS equipped with a He-Ne laser ( $\lambda = 633 \text{ nm}$ ), using folded capillary cells (DTS1070). Optical absorption spectra were acquired in a UV 6300PC spectrophotometer (VWR, Radnor, PA, USA).

#### 2.8. Antibacterial activity of AgNPs

The antibacterial assays of AgNPs were assessed by using the Kirby Bauer method [41] against human pathogenic Gram-positive (*Staphylococcus aureus*) and Gram-negative (*Escherichia coli*) bacteria grown in Mueller-Hinton agar medium at 37 °C for 24 h. Freshly cultured bacterial colonies of tested pathogens were taken, and 0.05 ml of inoculum was spread on each Mueller-Hinton agar plates. Sterile Whatman filter paper disks (6 mm diameter) were loaded with 2, 4 and 8  $\mu\text{g ml}^{-1}$  of AgNPs. The plant extract, antimicrobial susceptibility test discs (vancomycin, 5  $\mu\text{g}$  and tetracycline 10  $\mu\text{g}$  BD BBL Sensi-disc) and  $\text{AgNO}_3$  were used as the control in each plate and incubated at 37 °C for 24 h. The plates were examined for the presence of zones of inhibition, indicated by the clear area around the discs. The diameters of inhibition zones were measured, and the mean value for each organism was recorded.

### 3. Results and discussion

#### 3.1. Phytochemical screening of leaf extract

The phytochemical screening results for *P. florida* extract showed the presence of moderated content of flavonoids, as is observed in table 1. Flavonoids have been previously reported in plants of the *Parkinsonia* species [38]. Also, Orientin, vitexin, and epi-orientin have been reported in plants of the *Parkinsonia* species [33]. The screening results for *P. florida* extract also showed low content of saponins. These results are in concordance with other reports, where the presence of low content of saponins is observed, even using different solvents for extraction [42, 43]. By using different extraction methods and different solvents is possible to obtain different contents of the molecules of interest [38]. The results of the phytochemical analysis of *P. florida* extract

**Table 1.** Phytochemical screening assays for aqueous extracts from *P. florida*.

Component	<i>P. florida</i> extract
Alkaloids	NP
Carbohydrates	++
Saponins	+
Phenols	++
Flavonoids	++
Proteins	++
Cardiac glycosides	NP

+ = low content.

++ = moderate content.

NP = No presence.

**Table 2.** Antioxidant activity of *P. florida* leaf extract presented in Trolox Equivalents.

<i>P. florida</i> extract ( $\mu\text{g ml}^{-1}$ )	Equivalent trolox $\mu\text{g ml}^{-1}$
125	4.35
250	8.70
500	13.05
1000	17.40
2000	21.50

revealed the presence of moderated content of carbohydrates, phenols, and proteins. Besides, no cardiac glycosides were found in *P. florida* extract and also tested negative for the presence of alkaloids.

### 3.2. DPPH free radical scavenging activity

DPPH free radical scavenging activity was used to quantify the antioxidant content in *P. florida* leaf extract, and to secure the reproducibility in the nanoparticle synthesis, given that it is a complex mixture. DPPH reacts with H-donors groups that can serve as reducer agents. In this way, the evaluation of the antioxidant activity can serve as quality control during the reaction, avoiding the variations related to plant-to-plant or seasonal variation in antioxidants content. The data values of DPPH assay are presented in table 2; the *P. florida* leaf extract shows a logarithmic proportionality with the Trolox equivalents, as could be observed in figure 1S (supplemental information is available online at [stacks.iop.org/MRX/6/095025/mmedia](https://stacks.iop.org/MRX/6/095025/mmedia)). This result could help to predict the amount of equivalent Trolox from the extract concentration.

### 3.3. FT-IR analysis of leaf extract and nanoparticles

*P. florida* leaf extract and the metallic nanoparticles were analyzed with FT-IR to identify the possible biomolecules responsible for the formation, capping, and stabilization of the metallic nanoparticles. All the samples, including the leaf extract and the nanoparticles, presented intense bands at  $3209\text{ cm}^{-1}$ ,  $2932\text{ cm}^{-1}$ ,  $1580\text{ cm}^{-1}$ ,  $1392\text{ cm}^{-1}$ ,  $1282\text{ cm}^{-1}$ ,  $1073\text{ cm}^{-1}$  and  $843\text{ cm}^{-1}$ , related to different functional groups, as could be observed in figure 1. These bands corresponded to the adsorbed biomolecules on the surface of the nanoparticles. Given that the bands are presents both in nanoparticles and in the extract, it also indicates that the biomolecules influence on the formation of metallic nanoparticles and in their colloidal stabilization in the aqueous medium. The strong band observed at  $3209\text{ cm}^{-1}$  corresponds to the O–H stretching vibrations of carboxylic acids and phenolic groups. The peak at  $2932\text{ cm}^{-1}$  could be assigned to C–H stretching vibrations. The band observed at  $1580\text{ cm}^{-1}$  is identified as the amide I and arises due to the carbonyl stretch vibrations in the amide linkages of the proteins. The band observed at  $1385\text{ cm}^{-1}$  could be assigned to C–N stretching of nitrogen-containing compounds. The bands centered at  $1078\text{ cm}^{-1}$  and  $1023\text{ cm}^{-1}$  are assigned to C–OH vibrations and –C–O–C bending mode, respectively. The band at  $669\text{ cm}^{-1}$  might be the in-plane bending vibrations of N–H groups. These results indicated that specific biomolecules like phenols, proteins, aminoacids, saponins, and flavonoids present in *P. florida* leaf extract might have participated in the chemical reduction of the metallic salts and further colloidal stabilization. Also, the leaf extracts functional groups observed by FT-IR compared with the phytochemical screening results, support the role of surface modification with the presence of residues of phenols, proteins, aminoacids, saponins, and flavonoids. Flavonoids have functional groups that can actively chelate metal ions and can have an important role in the reduction of metals due to the tautomeric

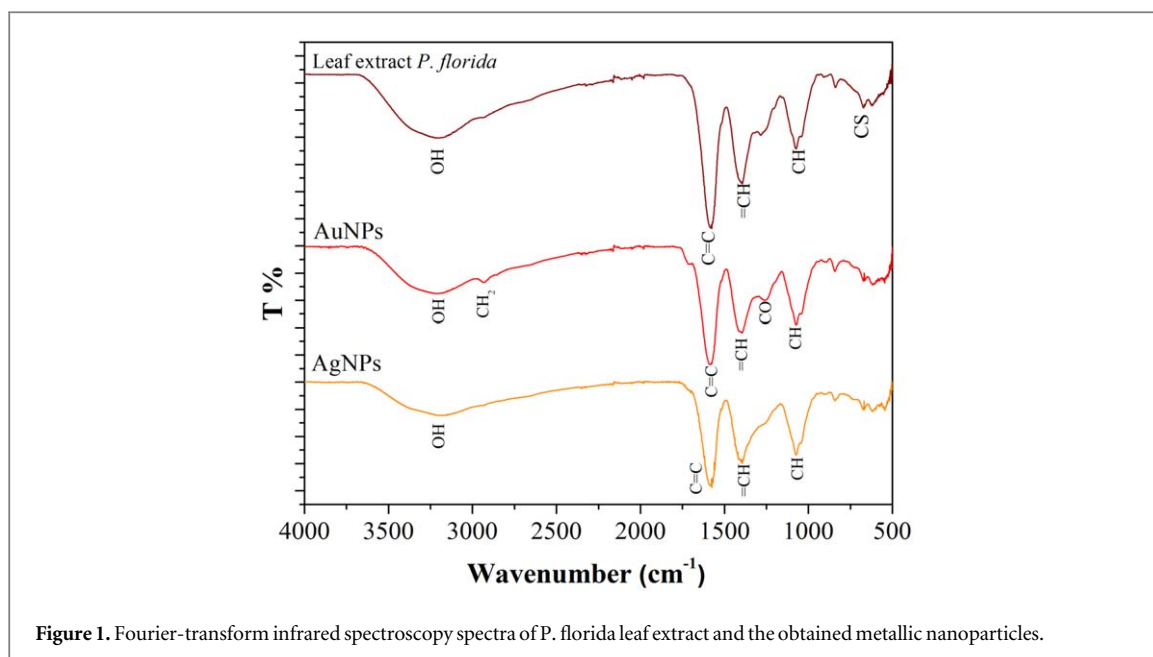


Figure 1. Fourier-transform infrared spectroscopy spectra of *P. florida* leaf extract and the obtained metallic nanoparticles.

transformations from the enol-form to the keto-form that may release a reactive hydrogen atom that can reduce metal ions [10]. Several amino acids can play a role of reducing agents in the formation of metallic nanoparticles and in the nanoparticle stabilization by binding to metal ions. This amino acid role has widely discussed and analyzed in the literature [10].

### 3.4. Nanoparticles characterization

Gold and silver nanoparticles exhibit characteristic colors in aqueous solutions due to excitation of surface plasmon vibrations. The reduction of gold and silver ions to form nanoparticles during exposure to plant leaf extracts could be followed through optical absorption spectroscopy [28]. Gold and silver nanoparticles exhibit ruby red and yellowish-brown color in water, respectively. Figure 2(a) shows the surface plasmon resonance bands for AuNPs prepared with *P. florida* leaf extract at different Equivalent Trolox. The maximum absorption peaks for AuNPs prepared in the range from 4.35 to 17.40  $\mu\text{g ml}^{-1}$  of equivalent Trolox are around 550 nm. A displacement of the absorbance band to 562 nm is observed when 21.50  $\mu\text{g ml}^{-1}$  of equivalent Trolox are used in the synthesis. Also, the intensity of the absorbance band is inversely proportional to the equivalent Trolox in the range from 4.35 to 17.40  $\mu\text{g ml}^{-1}$ . This behavior shows that by increasing the *P. florida* leaf extract concentration, the gold reduction is enhanced; thus, a reduced number of particles can be obtained but with larger diameters. When 21.50  $\mu\text{g ml}^{-1}$  of equivalent Trolox are used, an increase of the intensity of the absorbance band is observed, regarding the previous equivalent Trolox concentrations. This increase of the intensity might indicate that other morphologies or aggregations can arise at higher concentrations of the *P. florida* leaf extract. The surface plasmon resonance bands for AgNPs prepared at different Equivalent Trolox are presented in figure 2b. The maximum absorbance bands for AgNPs were in a close range from 444 to 462 nm, but the preparations with 8.70 to 17.40  $\mu\text{g ml}^{-1}$  of equivalent Trolox presented a maximum band around 462 nm. Also, in the same range of equivalent Trolox could be observed an inverse proportionality with the intensity of the absorption band. This behavior, also observed in the AuNPs synthesis, could be due to changes in the nanoparticle sizes as the equivalent Trolox rise. Additionally, at 21.50  $\mu\text{g ml}^{-1}$  of equivalent Trolox an increase of the intensity of the absorbance band, regarding the previous equivalent Trolox concentrations, is observed, and could also be explained in a similar way to AuNPs.

The absorption spectra of silver and gold nanoparticles in the region of the SPR wavelength were simulated by a Lorentzian distribution, according to Mie theory, as reported in the literature [44]. The unknown parameters were determined by a nonlinear regression algorithm from MATLAB® (MathWorks, USA). The Lorentzian fits for all the nanoparticles prepared in this work are presented in Fig. S2 (supporting information). Good correlation coefficients and similarities in the surface plasmon resonance bands between the experimental and the theoretical values were obtained for all preparations, as can be observed in table 3; these results indicate that Mie theory was suitable for analyzing the experimental data. The estimated width at half maximum correlates to the nanoparticle polydispersity; then, gold nanoparticles polydispersity increases with increasing concentration of equivalent Trolox (table 3). This result supports the notion stated before that different morphologies or aggregations arise at higher concentrations of the *P. florida* leaf extract. Similarly, the

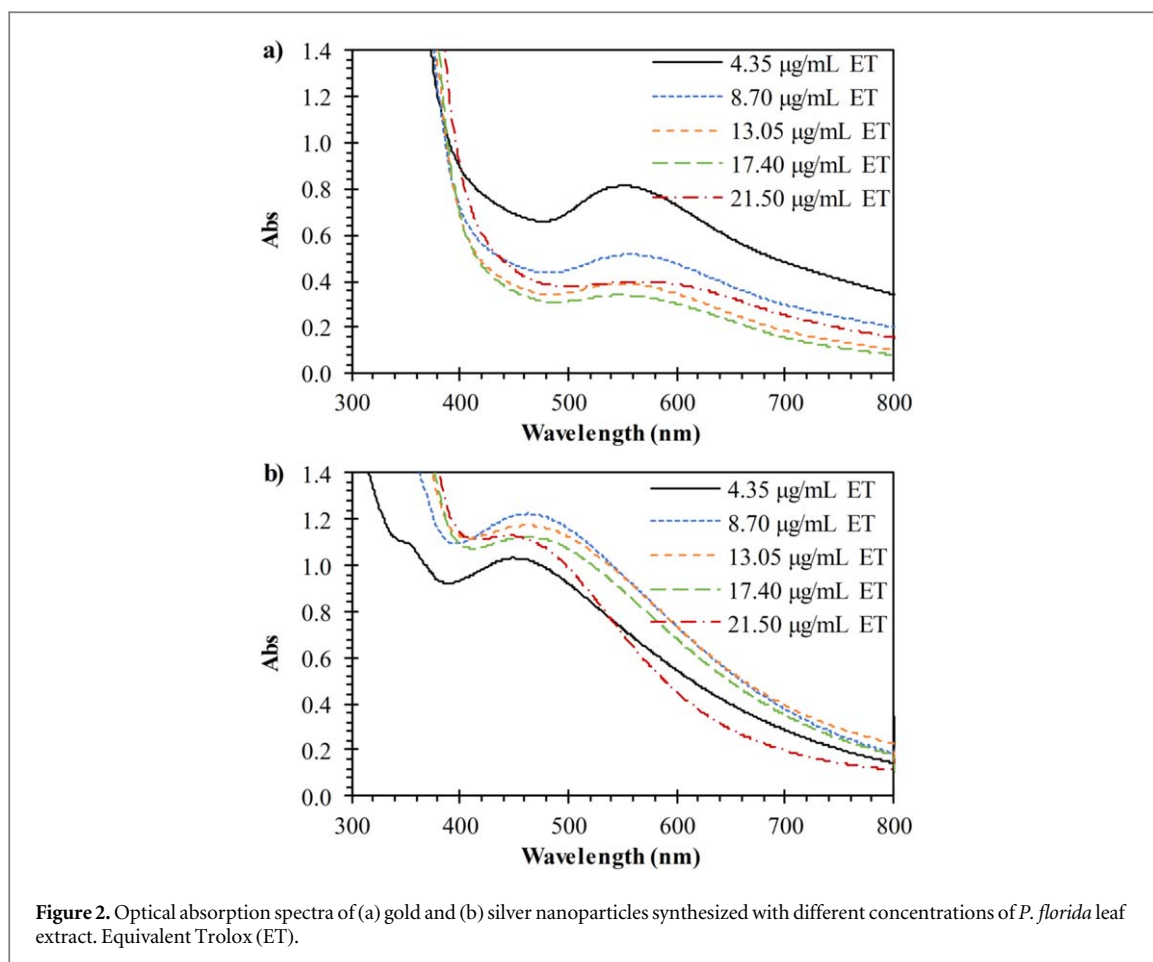


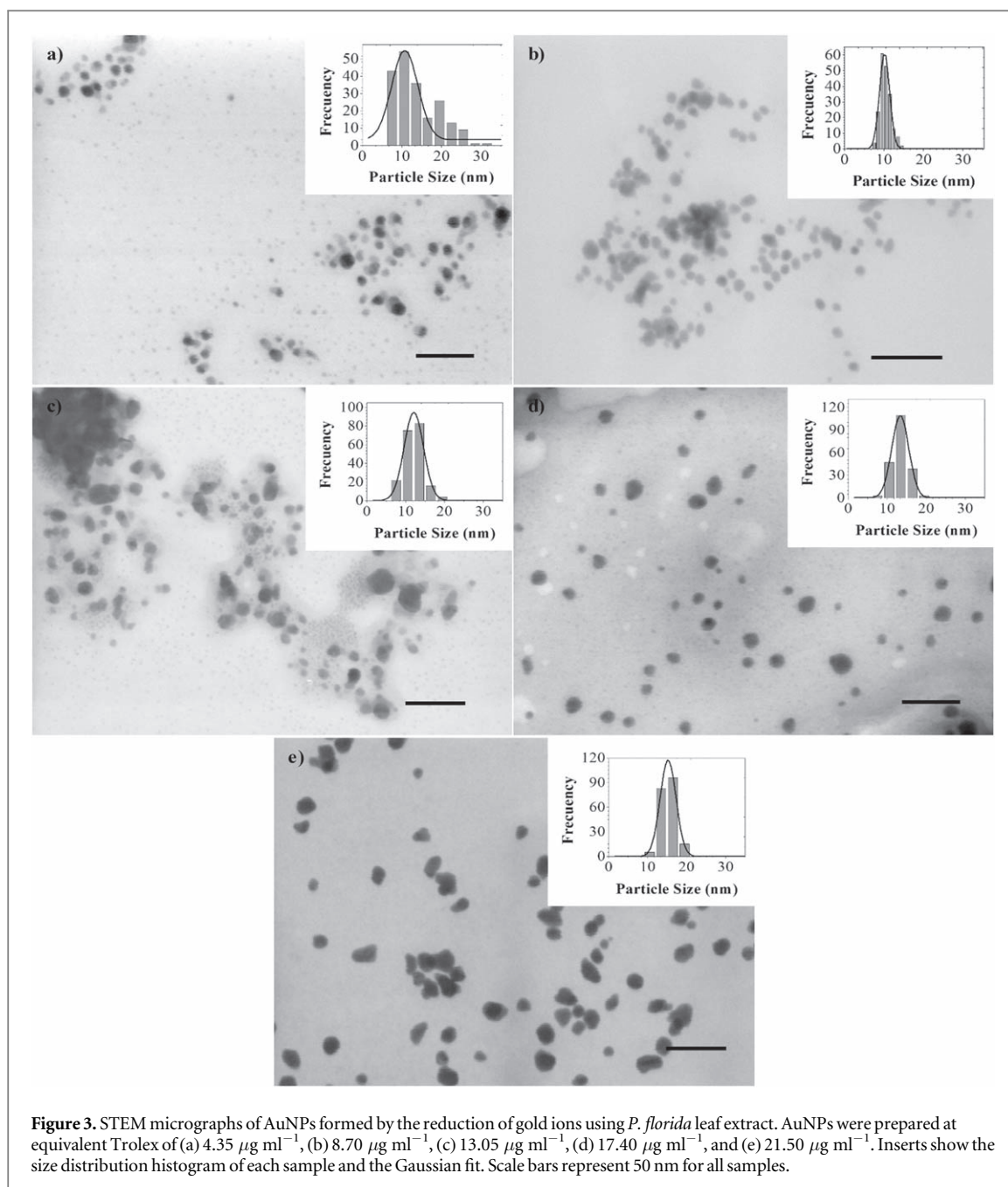
**Figure 2.** Optical absorption spectra of (a) gold and (b) silver nanoparticles synthesized with different concentrations of *P. florida* leaf extract. Equivalent Trolox (ET).

**Table 3.** Particle size diameter of gold and silver nanoparticles synthesized with *P. florida* leaf extract.

	Equivalent Trolox ( $\mu\text{g ml}^{-1}$ )	Peak plasmon resonance wavelength from experimental data (nm)	Peak plasmon resonance wavelength (nm) from Lorentzian fit	Width at half maximum from Lorentzian fit (nm)	Lorentzian fit correlation coefficient ( $R^2$ )	Average diameter size (nm) from STEM histograms
AuNPs	4.35	551	554	116.9634	0.9991	$11 \pm 3$
	8.70	557	556	132.8796	0.9995	$10 \pm 1$
	13.05	551	546	146.1463	0.9994	$12 \pm 2$
	17.40	546	543	157.3771	0.9990	$13 \pm 2$
	21.50	562	552	209.7456	0.9973	$15 \pm 2$
AgNPs	4.35	450	448	169.9689	0.9998	$17 \pm 2$
	8.70	462	462	183.5814	0.9999	$57 \pm 6$
	13.05	462	458	192.9360	0.9997	$47 \pm 2$
	17.40	461	456	195.1128	0.9997	$38 \pm 2$
	21.50	444	442	138.0952	0.9989	$10 \pm 1$

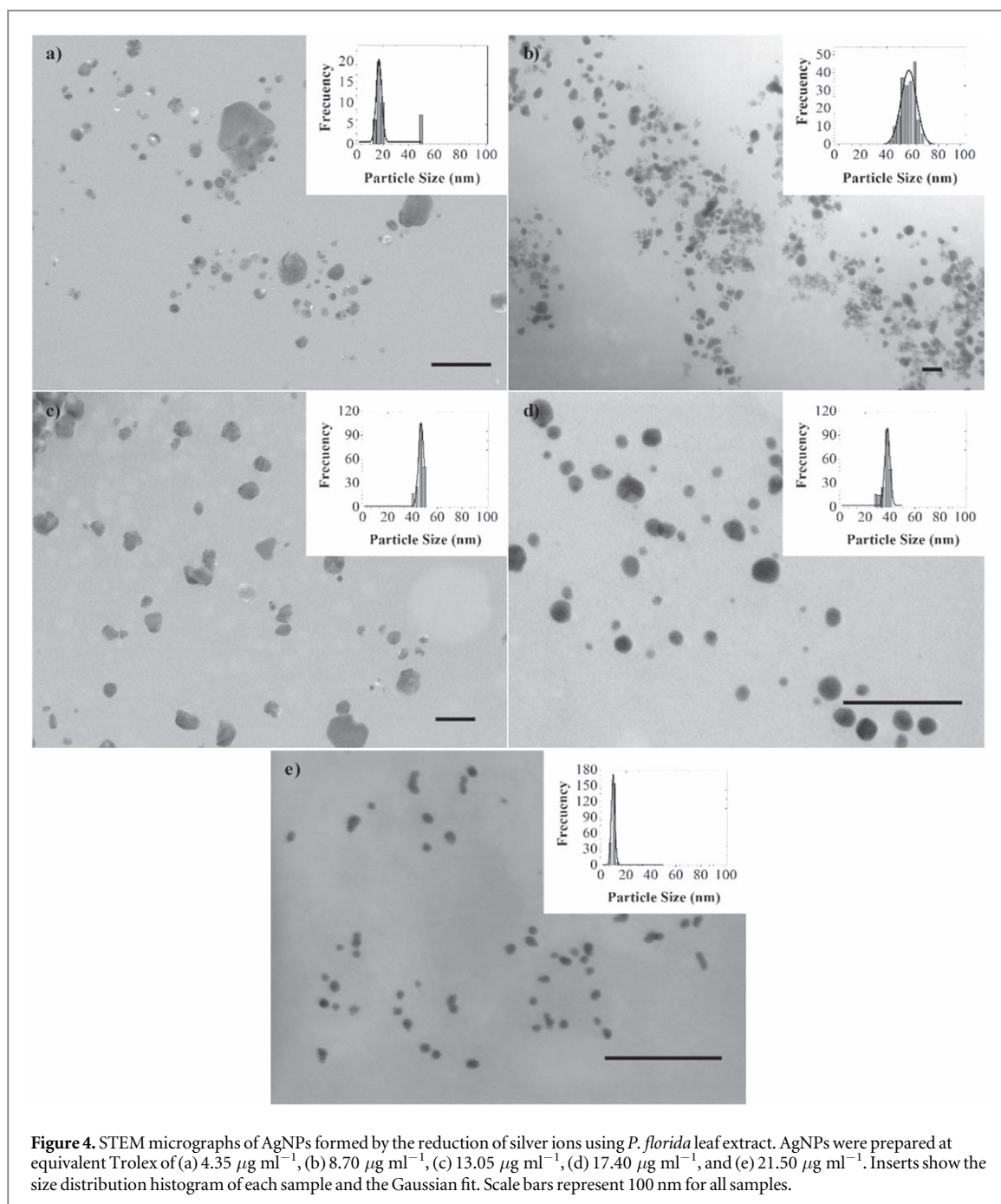
polydispersity of silver nanoparticles increased from  $4.35 \mu\text{g ml}^{-1}$  to  $17.40 \mu\text{g ml}^{-1}$ ; afterwards, at higher equivalent Trolox concentrations, the polydispersity of silver nanoparticles and the average diameter size decreases considerably as seen in table 3.

The STEM micrographs and histograms of AuNPs are presented in figure 3. The particles present quasi-spherical morphology. Histograms show that the diameter size of AuNPs is maintained within a close range for all preparations. Also, the polydispersity of AuNPs is low for all preparations, except for the ones prepared at  $4.35 \mu\text{g ml}^{-1}$  of equivalent Trolox, where a more size variations are observed. The average diameter of AuNPs was obtained by a Gaussian fit of histograms of figure 3, and are presented in table 3. The average diameters of AuNPs present a tendency to increase as the equivalent Trolox increase, but with no significant differences. Similar sizes have been reported for gold nanoparticles synthesized with aqueous and ethanolic aranto extracts, with mean diameters of  $7.7 \pm 2.0 \text{ nm}$  and  $17.5 \pm 5.3 \text{ nm}$  respectively [45].



The STEM micrographs and histograms of AgNPs are presented in figure 4. AgNPs present a quasi-spherical morphology for all preparations. The diameter sizes can be varied with extract concentration, as could be observed in table 3. The diameter size values were obtained from a Gaussian fit of the histograms of figure 4. The obtained nanoparticles tend to decrease its size as the concentration of the extract is increased, except for the less concentrated sample. As the concentration of the extract is increased, a more significant amount of particle nuclei is formed, resulting in reduced particle size. From the results mentioned above, it can be inferred that gold and silver nanoparticle formation follows different reaction mechanisms, a phenomenon that could be related to differences in valence and ionic radii of the metals. Silver nanoparticles with similar size were synthesized using *Brassica juncea* (mustard greens) and *Medicago sativa* (alfalfa) [10]. *Li et al* synthesized silver nanoparticles by treating silver ions with *Capsicum annum L.* extract obtaining AgNPs with a different size between 10 nm and 40 nm [46]. Xin-Huang *et al*, synthesized gold nanoparticles in the range of 7.2 to 12.8 nm [47] using bayberry tannin.

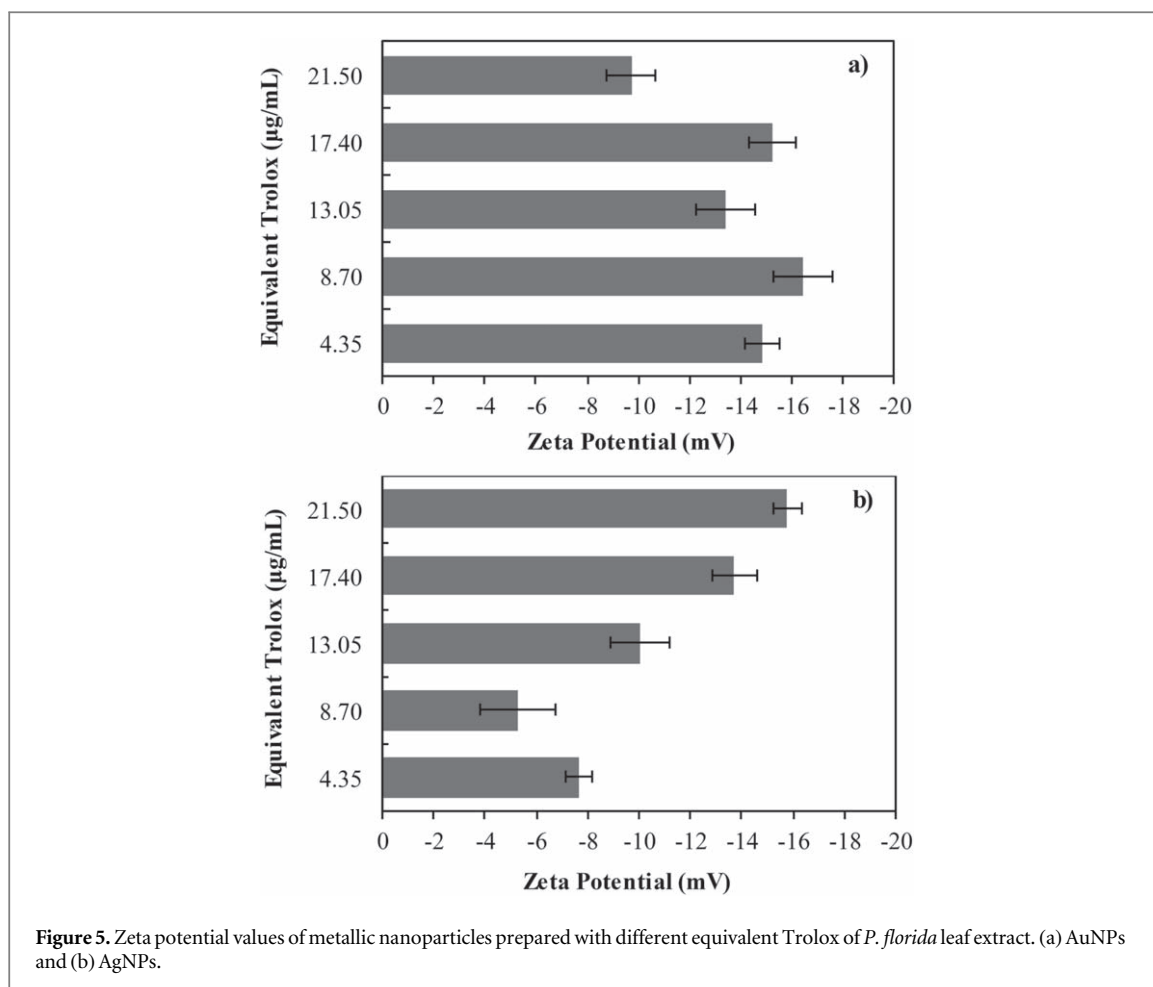
Based on the literature, other researchers have found using similar approaches that their synthesized nanoparticle structures follow a crystalline nature with face centered cubic lattice for gold [48, 49], and something along the same lines with also a face centered cubic lattice for silver [48, 50, 51]. Therefore, we expect to have a structure quite similar to the ones reported in the literature, since the processes of synthesis are similar.



Zeta potential measurements were carried out 24 h after particle synthesis, and the results are presented in figure 5. AuNPs presented negative zeta potential values in the range of  $-10 \pm 1$  to  $-16 \pm 1$  mV. These results are similar to other studies preparing AuNPs using leaf extracts [52]. Zeta potential values of AuNPs are variable and do not present trend respect the concentration of extract utilized in the synthesis, similar to the results obtained from STEM analysis.

Similarly, AgNPs samples presented negative zeta potential values in the range of  $-5 \pm 1$  to  $-16 \pm 1$  mV. Zeta potential values of AgNPs tend to decrease as the concentration of *P. florida* leaf extract increases. This effect can be related to an increase in the number of nucleation sites for the nanoparticle formation; leading to a more significant number of nanoparticles than with less extract, but with smaller diameters (as could be verified in table 3). Then, nanoparticles with the larger surface area are obtained by using more leaf extract, and more molecules could be adsorbed on the surface, increasing its net charge and enhancing its colloidal stability. Similar results were reported by Heydari and Rashidipour when AgNPs were prepared with extract of *oak fruit hull* ( $-25.3$  mV) [53]. Silver nanoparticles synthesized using *Calliandra haematocephala* leaf extract showed a zeta potential value of  $-17.2$  mV [54], and a zeta potential value of  $-24.1$  mV was reported from AgNPs synthesized using leaf extract of *Urtica dioica* Linn [55]. The negative charge obtained through these methods





cannot be explained with certainty, due to the presence of several molecules in the extracts that have not been identified and its characterization is far from the scope of this work. Though the FTIR discussed in figure 2 shows the presence of C-S bonds, these groups usually indicate the presence of thiol-like functional groups; which at certain pH can be deprotonated inducing the Zeta potential shift into the negative region as well as other molecules from the extract [56].

### 3.5. Antibacterial activity assay of silver nanoparticles

The antibacterial activity of AgNPs was investigated against *S. aureus* and *E. coli* using the agar disk diffusion method. The diameter of the inhibition zone (millimeter) is shown in (Table 4) and (figure 6). In the present study, the zone of inhibition for AgNPs was found to be 12 mm against *S. aureus* and 7.8 mm for *E. coli*. Leaf extract of *P. florida* does not show antibacterial activity against Gram-positive or Gram-negative bacteria. On the other hand, AgNPs showed better antibacterial activity compared to AgNO<sub>3</sub> solution. The AgNPs exhibited good antibacterial activity against *S. aureus* and lower antibacterial activity against *E. coli* (table 4, figure 6).

The inhibitory action of the metallic nanoparticles on microorganisms it is not well defined, it is suggested that the antibacterial activity can be possible due to Ag<sup>+</sup> released from AgNPs, acting as an antibacterial agent [57]. Feng *et al* proposed two antibacterial mechanisms of silver ions (1) silver ions can interact with thiol groups in proteins inactivating enzymatic activity and (2) silver ions can condense DNA molecules and make they lose their replication abilities [58]. Additionally, Li *et al* proposed an antimicrobial mechanism of AgNPs against *S. aureus*, their proposed that the particles probably can overpass the cell wall and interact with cell membrane to cripple some enzymes and interfere with normal metabolism of cells, afterward AgNPs enter into bacterial cells and condensed DNA to avoid DNA replication, avoiding cell reproduction. Finally, the interaction with cell wall and cell membrane destroy them, inducing bacterial death [59]. On the other hand, different reports in literature conclude that significant changes in the membrane structure of *E. coli* occur as a result of the interaction with silver ions, leading to an increase of permeability of the membrane and consequent death of the bacteria [58, 60].

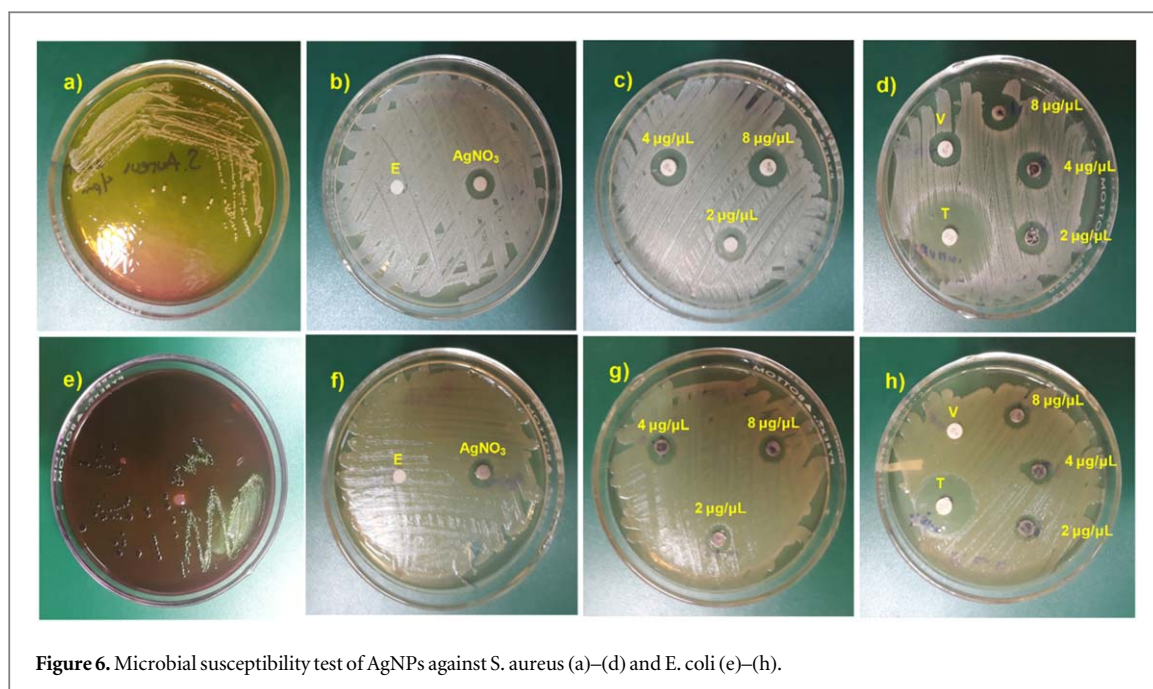


**Figure 6.** Microbial susceptibility test of AgNPs against *S. aureus* (a)–(d) and *E. coli* (e)–(h).

**Table 4.** Antimicrobial susceptibility test results.

Pathogen	Inhibition zone diameter (mm)						
	Controls				AgNPs		
	Tetracycline (10 µg)	Vancomycin (5 µg)	<i>P. Florida</i> Extract (8 µg µl <sup>-1</sup> )	Silver nitrate (17 µg µl <sup>-1</sup> )	8 µg µl <sup>-1</sup>	4 µg µl <sup>-1</sup>	2 µg µl <sup>-1</sup>
<i>S. aureus</i>	33	10	0	9.3	12.5	11.7	10.5
<i>E. coli</i>	27	0	0	7.2	7.8	6.5	5

## 4. Conclusions

This work describes a method for the preparation of gold and silver nanoparticles colloids using *P. florida* leaf extract as a reducing and stabilizing agent. The extract is an active reducing agent to form metallic nanoparticles at room temperature without any additional reagent or treatment. Biomolecules like aminoacids, saponins, and flavonoids present in *P. florida* leaf extract may have participated in the chemical reduction of the metallic salts and further colloidal stabilization. The biosynthesis is efficient and reproducible and shows potential for practical applications. The synthesized AgNPs showed good antibacterial activity compared to conventional antibiotics against *S. aureus* and *E. coli*. The method of synthesis of AgNPs and AuNPs using *P. florida* leaves extract is eco-friendly and straightforward.

## 5. Uncited references

[26]; [ is found mainly in the Colorado desert, the southeast of California, the Sonora desert, southern Arizona, and in the northwest of the state of Sonora (Mexico [

## Acknowledgments

Financial support of National Council of Science and Technology (CONACyT) through grant numbers INFR-226208–2014 and INFR-255791-2015 are appreciated. ALM thanks CONACyT for the doctoral fellowship awarded.

## ORCID iDs

Roberto Carlos Carrillo-Torres  <https://orcid.org/0000-0002-1295-5168>

Reynaldo Esquivel  <https://orcid.org/0000-0002-8546-8619>

Armando Lucero-Acuña  <https://orcid.org/0000-0002-2331-9351>

## References

- [1] Frens G 1973 Controlled nucleation for the regulation of the particle size in monodisperse gold suspensions *Nat Phys Sci* **241** 20–2
- [2] Prevo B G et al 2008 Scalable routes to gold nanoshells with tunable sizes and response to near-infrared pulsed-laser irradiation *Small* **4** 1183–95
- [3] Liang C et al 2011 Improved therapeutic effect of folate-decorated PLGA-PEG nanoparticles for endometrial carcinoma *Bioorgan Med Chem* **19** 4057–66
- [4] Sengani M, Grumezescu A M and Rajeswari V D 2017 Recent trends and methodologies in gold nanoparticle synthesis—A prospective review on drug delivery aspect *OpenNano* **2** 37–46
- [5] Mohammadlou M, Maghsoudi H and Jafarizadeh-Malmiri H 2016 A review on green silver nanoparticles based on plants: synthesis, potential applications and eco-friendly approach *Int Food Res J* **23** 446–63
- [6] Islam A, Bhuiya M A K and Islam M S 2014 A Review on Chemical Synthesis Process of Platinum Nanoparticles. *Asia Pacific J Energy Environ* **1** 107–21
- [7] Mishra V et al 2014 International journal of green and a review on green synthesis of nanoparticles and evaluation of antimicrobial activity *Int J Green Herb Chem* **3** 81–94
- [8] Kameswara Srikar S et al 2016 Green synthesis of silver nanoparticles: a review *Green Sustain Chem* **6** 34–56
- [9] Mohanpuria P, Rana N K and Yadav S K 2008 Biosynthesis of nanoparticles: technological concepts and future applications *J Nanoparticle Res* **10** 507–17
- [10] Makarov V V et al 2014 "Green" nanotechnologies: synthesis of metal nanoparticles using plants *Acta Naturae* **6** 35–44
- [11] Nadagouda M N and Varma R S 2008 Green synthesis of silver and palladium nanoparticles at room temperature using coffee and tea extract *Green Chem.* **10** 859–62
- [12] Anastas P T, Heine L G and Williamson T C 2000 *Green Chemical Syntheses and Processes* (Washington DC: American Chemical Society)
- [13] Jayaseelan C et al 2013 Green synthesis of gold nanoparticles using seed aqueous extract of *Abelmoschus esculentus* and its antifungal activity *Ind. Crops Prod.* **45** 423–9
- [14] Shankar S S et al 2004 Rapid synthesis of Au, Ag, and bimetallic Au core-Ag shell nanoparticles using Neem (*Azadirachta indica*) leaf broth *J. Colloid Interface Sci.* **275** 496–502
- [15] Elia P et al 2014 Green synthesis of gold nanoparticles using plant extracts as reducing agents *Int J Nanomedicine* **9** 4007–21
- [16] Albusta N et al 2018 Detection of glucose using gold nanoparticles prepared by green synthesis *Int J Eng Sci Res* **6** 1–10
- [17] Vijayan R, Joseph S and Mathew B 2017 Indigofera tinctoria leaf extract mediated green synthesis of silver and gold nanoparticles and assessment of their anticancer, antimicrobial, antioxidant and catalytic properties *Artif Cells, Nanomedicine, Biotechnol* **46** 861–71
- [18] Khan A et al 2014 Gold Nanoparticles: synthesis and applications in drug delivery *Pharm Res Trop J Pharm Res J Cit Reports Science Ed* **13** 1169–1169
- [19] Ghosh P et al 2008 Gold nanoparticles in delivery applications *Adv Drug Deliv Rev* **60** 1307–15
- [20] Iancu C 2013 Photothermal therapy of human cancers (PTT) using gold nanoparticles *Biotechnol Mol Biol Nanomedicine* **1** 53–60
- [21] Huang X and El-Sayed M A 2010 Gold nanoparticles: optical properties and implementations in cancer diagnosis and photothermal therapy *J. Adv. Res.* **1** 13–28
- [22] Dreaden E C et al 2011 Beating cancer in multiple ways using nanogold *Chem. Soc. Rev.* **40** 3391–404
- [23] Loo C et al 2004 Nanoshell-enabled photonics-based imaging and therapy of cancer *Technol. Cancer Res. Treat.* **3** 33–40
- [24] Gao J et al 2012 Colloidal stability of gold nanoparticles modified with thiol compounds: bioconjugation and application in cancer cell imaging *Langmuir* **28** 4464–71
- [25] Aljabali A et al 2018 Synthesis of gold nanoparticles using leaf extract of *Ziziphus zizyphus* and their antimicrobial activity *Nanomaterials* **8** 174
- [26] Verma A and Mehata M S 2016 Controllable synthesis of silver nanoparticles using Neem leaves and their antimicrobial activity *J Radiat Res Appl Sci* **9** 109–15
- [27] Ibrahim H M M 2015 Science direct green synthesis and characterization of silver nanoparticles using banana peel extract and their antimicrobial activity against representative microorganisms *J Radiat Res Appl Sci* **8** 265–75
- [28] Geethalakshmi R and Sarada D V L 2010 Synthesis of plant-mediated silver nanoparticles using *Trianthema decandra* extract and evaluation of their anti microbial activities *Int J Eng Sci Technol* **2** 970–5
- [29] Chandirikia U and Annadurai G 2018 Biosynthesis and characterization of silver nanoparticles using leaf extract *abutilon indicum* *Glob J Biotechnol Biochem* **13** 07–11
- [30] Wang L et al 2018 Characterization, antioxidant and antimicrobial activities of green synthesized silver nanoparticles from *Psidium guajava* L. leaf aqueous extracts *Mater. Sci. Eng. C* **86** 1–8
- [31] Kailasa S K et al 2018 Antimicrobial activity of silver nanoparticles *Nanoparticles in Pharmacotherapy* (Elsevier Inc) 461–84
- [32] Divya B, Mruthunjaya K and Manjula S N 2011 Parkinsonia aculeata: a phytopharmacological review *Asian J Plant Sci* **10** 175–81
- [33] Bhatia V K, Gupta S R and Seshadri T R 1966 C-Glycosides of the leaves of *Parkinsonia aculeata* *Tetrahedron* **22** 1147–52
- [34] Khan A S 2017 Leguminous Trees and Their Medical Properties *Medicinally Important Trees* (eBook: Springer) 211–30
- [35] Andrade-Cetto A and Heinrich M 2005 Mexican plants with hypoglycaemic effect used in the treatment of diabetes *J. Ethnopharmacol.* **99** 325–48
- [36] Prashant Tiwari B, Kumar M K and Gurpreet Kaur H K 2011 Phytochemical screening and extraction—a review *Int Pharm Sci* **1** 98–106
- [37] Cheel J et al 2010 Free radical-scavenging, antioxidant and immunostimulating effects of a licorice infusion (*Glycyrrhiza glabra* L.) *Food Chem.* **122** 508–17
- [38] Ahmed S et al 2016 Green synthesis of silver nanoparticles using *Azadirachta indica* aqueous leaf extract *J Radiat Res Appl Sci* **9** 1–7
- [39] Hudzicki J 2009 Kirby-bauer disk diffusion susceptibility test protocol. *Am Soc Microbiol* 1–23

- [42] Hungund B L and Pathak C H 1971 A Survey of Plants in Gujarat, India, for Alkaloids, Saponins, and Tannins 1–11
- [43] Sharma S and Vig A P 2014 Preliminary phytochemical screening and *in vitro* antioxidant activities of *Parkinsonia aculeata* linn *Biomed Res Int* **2014** 1–8
- [44] Baset S et al 2011 Size measurement of metal and semiconductor nanoparticles using UV–vis absorption spectra *Dig J Nanomater Biostructures* **6** 709–16
- [45] Vergara-castañeda H et al 2019 Gold nanoparticles bio-reduced by natural extracts of arantho (*Kalanchoe daigremontiana*) for biological purposes: physicochemical, antioxidant and antiproliferative evaluations *Mater Res Express Pap* **6** 055010
- [46] Li S et al 2007 Green synthesis of silver nanoparticles using *Capsicum annuum* L. extract *Green Chem.* **9** 852
- [47] Huang X et al 2010 One-step, size-controlled synthesis of gold nanoparticles at room temperature using plant tannin *Green Chem.* **12** 395
- [48] Francis S et al 2017 Green synthesis and characterization of gold and silver nanoparticles using *Mussaenda glabrata* leaf extract and their environmental applications to dye degradation *Environ Sci Pollut Res* **24** 17347–57
- [49] Chahardoli A et al 2018 Green approach for synthesis of gold nanoparticles from *Nigella arvensis* leaf extract and evaluation of their antibacterial, antioxidant, cytotoxicity and catalytic activities *Artif Cells, Nanomedicine Biotechnol* **46** 579–88
- [50] Irvani S 2011 Green synthesis of metal nanoparticles using plants *Green Chem.* **13** 2638–50
- [51] Siddiqi K S, Husen A and Rao R A K 2018 A review on biosynthesis of silver nanoparticles and their biocidal properties *J Nanobiotechnology* **16** 1–28
- [52] Adavallan K and Krishnakumar N 2014 Mulberry leaf extract mediated synthesis of gold nanoparticles and its anti-bacterial activity against human pathogens *Adv. Nat. Sci.: Nanosci. Nanotechnol.* **5** 1–9
- [53] Heydari R and Rashidipour M 2015 Green synthesis of silver nanoparticles using extract of oak fruit hull (Jaft): synthesis and *in vitro* cytotoxic effect on MCF-7 cells *Int J Breast Cancer* **2015** 1–6
- [54] Raja S, Ramesh V and Thivaharan V 2017 Green biosynthesis of silver nanoparticles using *Calliandra haematocephala* leaf extract, their antibacterial activity and hydrogen peroxide sensing capability *Arab J Chem* **10** 253–61
- [55] Jyoti K, Baunthiyal M and Singh A 2016 Characterization of silver nanoparticles synthesized using *Urtica dioica* Linn. leaves and their synergistic effects with antibiotics *J Radiat Res Appl Sci* **9** 217–27
- [56] Thielbeer F, Donaldson K and Bradley M 2011 Zeta potential mediated reaction monitoring on nano and microparticles *Bioconjug Chem* **22** 144–50
- [57] Kaviya S et al 2011 Biosynthesis of silver nanoparticles using citrus sinensis peel extract and its antibacterial activity *Spectrochim Acta Part A Mol Biomol Spectrosc* **79** 594–8
- [58] Feng Q L et al 2000 A mechanistic study of the antibacterial effect of silver ions on *Escherichia coli* and *Staphylococcus aureus* *J Biomed Mater Res banner* **52** 662–8
- [59] Li W-R et al 2011 Antibacterial effect of silver nanoparticles on *Staphylococcus aureus* *Biometals* **24** 135–41
- [60] Sondi I and Salopek-Sondi B 2004 Silver nanoparticles as antimicrobial agent: a case study on *E. coli* as a model for Gram-negative bacteria *J. Colloid Interface Sci.* **275** 177–82